

# Fiber-Fiber Coefficient of Friction: Effects of Modulus and $\tan \delta$

D. C. PREVORSEK and R. K. SHARMA, *Chemical Research Center, Allied Chemical Corporation, Morristown, New Jersey 07960*

## Synopsis

The technologically important studies on rubber friction and wear give strong support to rubber friction being a viscoelastic phenomenon. However, the basic concepts and conclusions derived from such studies appear to have general validity. Fiber-to-fiber friction studies are carried out on a number of polymeric filaments with a view to establishing the relationships between fundamental mechanical properties such as modulus,  $\tan \delta$ , and the coefficient of friction. The relationship between these three quantities is expressed by an equation. The results show that with these fibers adhesive contribution to friction is negligible and that temperature and humidity variations in end uses have a much more important effect in frictional properties than changes in draw ratio, heat setting, and so on.

## INTRODUCTION

Considerable progress has been made in recent years in the understanding of friction and wear. Much of the work in this area concerned the technologically important problem of rubber friction and wear of pneumatic tires. Work on rubber friction at various temperatures, as function of sliding velocity has been shown, e.g., to give strong evidence for rubber friction being a viscoelastic phenomenon.<sup>1</sup> Since there is a similarity between the rolling friction and fiber-to-fiber friction measured by Gralen's technique,<sup>2</sup> we speculated that similar relationship could describe both phenomena, especially when fiber friction is measured above or near the glass transition temperature of the fiber. This is the case with nylon 6, nylon 12, and polypropylene fibers under ambient conditions.

The results of friction studies have been explained by the existence of two fundamentally different friction mechanisms. One of them is molecular "adhesion" between two surfaces<sup>3-6</sup>; it is the only mechanism of friction on a smooth track such as glass. The other process is mechanical energy loss due to gross deformations of the surfaces in contact<sup>7-10</sup>; this, for example, is the mechanism of friction on a lubricated track.<sup>11</sup> The adhesive theories of friction rely on expressions for the making and breaking of molecular bonds as separately activated processes. The formation of bonds is assumed to be due to local energy fluctuations of sufficient magnitude to surmount the activation energy barrier. The deformation theories of friction, on the other hand, examine the mechanical losses and the size of the domains that undergo deformation during a friction experiment.

It can be assumed that a realistic theory of friction must be concerned with both of these factors. Therefore, it was desirable to make an attempt to establish the relative importance of these two effects in fiber-to-fiber friction, or at least to design an experiment which could resolve these two contributions. In addi-

tion, we hoped that such a study will provide an explanation why changes in fiber processing conditions (i.e., changes in draw ratio, heat treatments, etc.) that significantly affect fiber modulus have a much smaller effect on the fiber-to-fiber coefficient of friction.

## EXPERIMENTAL

### Measurement of Fiber-to-Fiber Friction

The apparatus used was based on Lindberg's<sup>2</sup> principle illustrated in Figure 1. If two monofilaments are twisted together and the ends held under tension as shown, with  $P_1$  constant and  $P_2$  slowly increased, the conditions for the monofilaments to slip past each other are

$$P_1 \exp(\pi n \beta \mu) = P_2 \quad (1)$$

where  $n$  = number of twists,  $\beta = \pi/2$ -helix angle, and  $\mu$  = coefficient of friction. From this the parameter  $\mu$  is easily obtained. The apparatus is shown in Figure 2. The forces  $P_1$  were provided by the weights, as shown, and the load cell measured the force  $P_2$ . A great deal of care was given to make the rolling resistance of the pulleys as low as possible. The whole apparatus was enclosed in a constant-temperature and -humidity box.

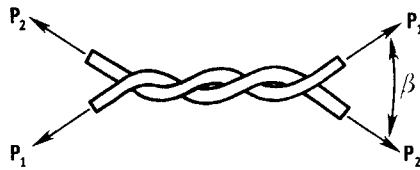


Fig. 1. Illustration of Lindberg's method for measuring fiber-to-fiber friction.

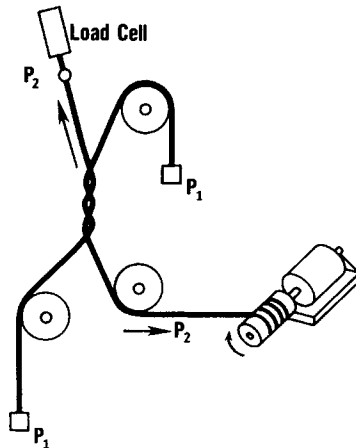


Fig. 2. Fiber-to-fiber friction apparatus.

### Measurement of Bending Moduli E

Young's modulus of materials obtainable in the form of slender bars or rods can be measured by determining the resonance frequency for the bar clamped at one end and vibrating as a reed. This method has the advantage of being nondestructive and applicable to very small samples. In the derivation of expression to calculate the modulus, it is assumed that Young's modulus is equal in tension and in compression. The frequency  $\nu_n$  of a bar vibrating in the  $n$ th harmonic is given by<sup>12</sup>

$$\nu = \frac{\pi \beta_n^2 [(Ek^2/\rho)^{1/2}]}{2L^2} \quad (2)$$

where  $L$  = length of the sample (cm),  $\rho$  = density of material ( $\text{g/cm}^3$ ),  $E$  = Young's modulus ( $\text{dynes/cm}^2$ ), and  $\beta_n$  is a dimensionless constant for the  $n$ th harmonic whose values are  $\beta_1 = 0.597$ ,  $\beta_2 = 1.494$ ,  $\beta_3 = 2.500$ , etc.  $k$  is a radius of gyration of the cross section; for a circle it is  $d/4$ , where  $d$  is the diameter.

A convenient procedure is to measure the resonance frequency for different values of  $L$  and then to plot frequency versus  $L^{-2}$ . The resulting straight line, for a fiber of circular cross section vibrating in the fundamental mode, has a slope equal to

$$0.125\pi d\beta^2[(E/\rho)^{1/2}]$$

or

$$0.140[(d^2E/\rho)^{1/2}]$$

where

$$E = 51 \times \text{slope}^2 \times d^{-2} \times \rho \quad \text{dynes/cm}^2$$

Vibrations were induced by electrostatic method. The apparatus and procedure of measurement have been described in detail elsewhere.<sup>13</sup>

### Measurement of Dynamic Mechanical Properties

Measurements of  $\tan \delta$  as a function of temperature and specific humidity were made by using a Vibron dynamic viscoelastometer. Humidity control was achieved by modifying the Vibron temperature chamber to allow injection of air of known relative humidity (at room temperature, 23°C). The moisture content of injected stream of air was controlled by mixing known proportions of saturated and dry air at 23°C. The temperature was monitored by a thermocouple placed about 2 mm from the center of the test specimen to provide temperature measurements to  $\pm 0.5^\circ\text{C}$ . Experiments to determine the variation of properties with temperature were made by increasing the temperature at constant heating rates of  $1^\circ\text{--}2^\circ\text{C/min}$  from the minimum to the maximum temperature employed. The average tensile strain used in the experiments varied from 0.1% to 0.5%. The tension of the sample was adjusted to each measurement point to allow for thermal expansion and contraction. The sinusoidal driving frequency used in the experiments was 110 cps.

## RESULTS

The experimental results obtained with nylon 6, poly(ethylene terephthalate), polypropylene, and nylon 12 yarns are shown in Figures 3-7.

Figure 3(a) shows the variation of modulus  $E$  and coefficient of friction  $\mu$  for nylon 6 yarn over a temperature range of  $-20^{\circ}$  to  $75^{\circ}\text{C}$  and a relative humidity of 65%, whereas the variation of  $\tan \delta$  under same conditions is shown in Figure 3(b). The variation of  $E$ ,  $\mu$ , and  $\tan \delta$  with relative humidity ranging from 0 to 100% and at a temperature of  $30^{\circ}\text{C}$  for nylon 6 yarn is shown in Figures 4(a) and 4(b). At constant relative humidity, both  $\mu$  and  $\tan \delta$  show a slight decrease with temperature change from about  $-20^{\circ}$  to about  $10^{\circ}\text{C}$ . This is followed by a monotonic increase in their values up to the upper end of the temperature of measurement,  $80^{\circ}\text{C}$ . The modulus  $E$ , on the other hand, does not show any significant change up to about  $20^{\circ}\text{C}$  and then decreases progressively with temperature. At  $30^{\circ}\text{C}$  both  $\tan \delta$  and  $\mu$  increase with relative humidity, with a tendency toward leveling off as the humidity increases to the saturation values. The modulus  $E$  decreases continuously as the humidity increases from 0% to 100%.

In the case of PET yarn, variation of  $\mu$  and  $E$  with temperature, as shown in Figure 5(a), is qualitatively similar to that with nylon 6 except that here the increase in  $\mu$  with temperature is much slower and the decrease in  $E$  with increase in temperature is more rapid.  $\tan \delta$ , Figure 5(b), decreases from about  $-25^{\circ}$ – $45^{\circ}\text{C}$  and then increases with increase in temperature.

The data of polypropylene yarn plotted in Figures 6(a) and 6(b) show trends

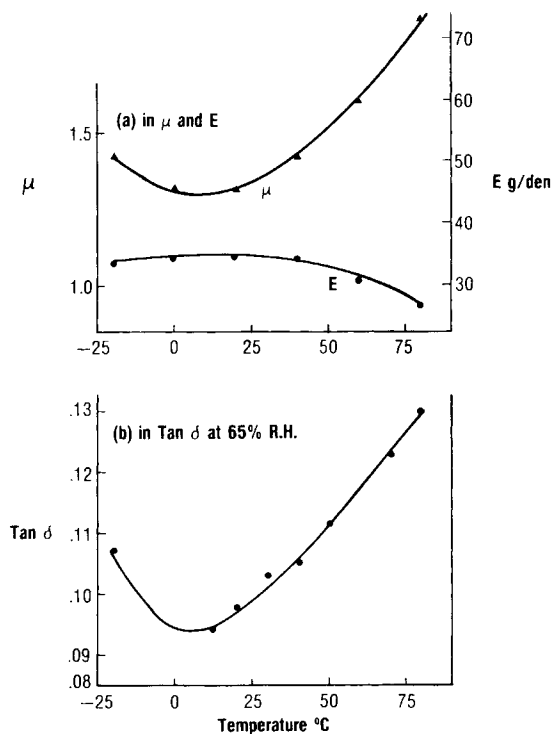


Fig. 3. Variation with temperature (a) in  $\mu$  and  $E$ ; (b) in  $\tan \delta$  for nylon 6 yarn at 65% R.H. Maximum strain rates for  $\tan \delta = 0.7$ – $3.5$ ,  $\mu = 3.5$ – $5.1$ , and  $E = 300$ – $450 \text{ sec}^{-1}$ .

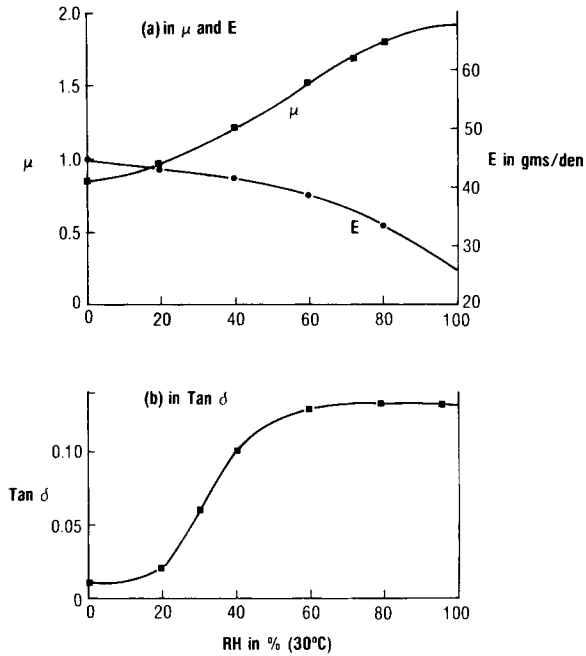


Fig. 4. Variation with humidity (a) in  $\mu$  and  $E$ ; (b) in  $\tan \delta$  for nylon 6 yarn at 30°C. Maximum strain rates for  $\tan \delta = 0.7-3.5$ ,  $\mu = 3.5-5.1$ , and  $E = 300-450 \text{ sec}^{-1}$ .

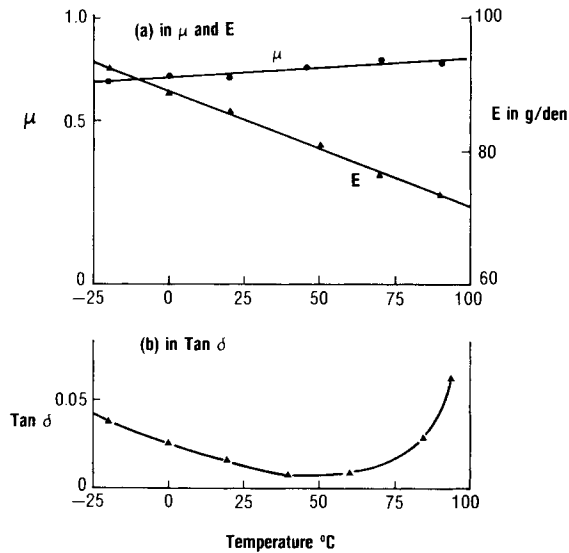


Fig. 5. Variation with temperature (a) in  $\mu$  and  $E$ ; (b) in  $\tan \delta$  for PET yarn. Maximum strain rates for  $\tan \delta = 0.7-3.5$ ,  $\mu = 3.5-5.1$ , and  $E = 300-450 \text{ sec}^{-1}$ .

similar to the other two yarns in that  $\mu$  increases with temperature and sonic velocity  $V$ , which is proportional to modulus, decreases with temperature.  $\tan \delta$  shows a maximum at about 45°C. Sonic velocity  $V$ , in m/sec, is converted to the modulus  $E$ , in g/den, from the relation

$$E = \rho \frac{(100V)^2}{980} \cdot \frac{1}{900,000\rho} = \frac{V^2}{90 \times 980}$$

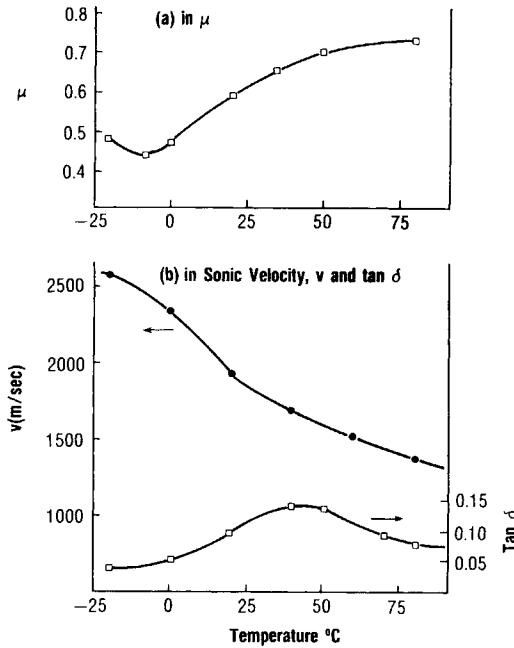


Fig. 6. Variation with temperature (a) in  $\mu$ ; (b) in sonic velocity  $V$  and  $\text{tan } \delta$  polypropylene yarn. Maximum strain rates for  $\text{tan } \delta = 0.7\text{--}3.5$ ,  $\mu = 3.5\text{--}5.1$ , and  $E = 300\text{--}450 \text{ sec}^{-1}$ .

where  $\rho$  is the density, in  $\text{g/cm}^3$ .

The results for nylon 12, plotted in Figures 7(a) and 7(b), show trends similar to those for nylon 6. At constant relative humidity of 65%,  $\mu$  and  $\text{tan } \delta$  show a slight decrease from  $-10^{\circ}$  to  $20^{\circ}\text{C}$ . This is followed by a monotonic increase in their values with increasing temperature. The modulus  $E$ , on the other hand,

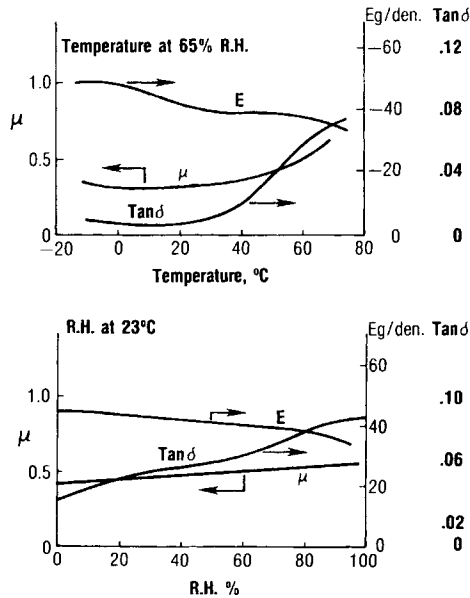


Fig. 7. Variation in  $\mu$ ,  $E$ , and  $\text{tan } \delta$  (a) with temperature at 65% R.H.; (b) with R.H. at  $23^{\circ}\text{C}$  for nylon 12 yarn. Maximum strain rates for  $\text{tan } \delta = 0.7\text{--}3.5$ ,  $\mu = 3.5\text{--}5.1$ , and  $E = 300\text{--}450 \text{ sec}^{-1}$ .

decreases with temperature throughout the temperature range studied. The variation with relative humidity at a temperature of 23°C, plotted in Figure 7(b), shows continuous increase in  $\mu$  and  $\tan \delta$  and a decrease in  $E$  with relative humidity.

## DISCUSSION

In the analysis that follows we assume that the coefficient of friction can be expressed as the sum of the adhesive ( $\mu_a$ ) and the deformation ( $\mu_d$ ) contributions and that in the temperature and humidity interval of interest the changes in  $\mu_a$  for a given fiber are small in comparison with the changes in  $\mu_d$ .

Bulgin et al.<sup>14</sup> measured friction of various tread compounds on brass tracks of different roughness and found the coefficient of friction to pass through a maximum with a change of temperature or sliding velocity. The temperature dependence of friction was similar to that of the loss tangent. Plots of corresponding point of friction force against loss tangent, for various tread rubbers, showed a roughly straight-line relationship. Since the work loss of a given sample is a function of deformation volume, its value and therefore the frictional force can be assumed to depend upon the area of contact between the two surfaces. An indication of such a dependence is shown by the work of Galen,<sup>2</sup> who carried out friction measurements of smooth nylon fibers at different tensions and contact areas. The results indicate that the size of the contact area and the work loss associated with the deformation which takes place at the contact area of the two fibers affect the deformation contribution of friction  $\mu_d$ .

Consider two fibers sliding past one another under a constant normal force at the junction (Fig. 8). Note that it is possible to conduct this experiment in such a way that the contact area of fiber A remains unchanged while fiber B is subjected to a deformation wave which propagates with the speed of the moving fiber A. Consider now the moving deformation zone in the fiber B shown in Figure 9. The right side of fiber A is in close contact with the deformed fiber B. On the trailing side of A, on the other hand, there is a gap between fibers A and B, because the recovery of fiber B is not instantaneous as the pressure of A is released. As a result there is a component of force which opposes the sliding of the fiber A across fiber B. The work associated with this motion is proportional to the energy loss experienced while the deformation zone travels across the fiber B.

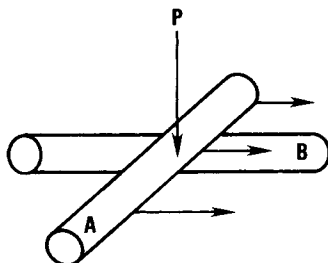


Fig. 8. Two fibers sliding past one another.



Fig. 9. Moving deformation zone in fibers sliding under normal force.

This energy loss is proportional to the volume of the deformation zone and the mechanical loss factor ( $\tan \delta$ ) of the fiber. Considering that the volume of the deformation zone is inversely correlated with fiber modulus  $E$ , it can be assumed that the coefficient of friction  $\mu$  can be described by the following relationship:

$$\mu(\epsilon, \dot{\epsilon}, T, \dots) = \mu_a + \mu_d = a + B \frac{\tan \delta^m(\epsilon, \dot{\epsilon}, T, \dots)}{E^n(\epsilon, \dot{\epsilon}, T, \dots)} \quad (3)$$

where the first member on the right side,  $\mu_a$ , represents the adhesive and second member,  $\mu_d$ , the deformation contribution and  $\epsilon$  and  $\dot{\epsilon}$  are strain and strain rate, respectively. It must be noted that  $\mu$ ,  $\tan \delta$ , and  $E$  are functions of strain amplitude  $\epsilon$ , strain rate  $\dot{\epsilon}$ , temperature  $T$ , and other factors such as relative humidity (R.H.). In order to establish the validity of eq. (3), it is therefore necessary to measure  $\mu$ ,  $E$ , and  $\tan \delta$  under the same conditions. With regard to  $T$  and R.H. there is no problem. Determination of  $\mu$ ,  $\tan \delta$  and  $E$ , however, involves three different methods, and therefore  $\epsilon$  and  $\dot{\epsilon}$  are not the same for all three variables. In order to establish the magnitude of error associated with differences in  $\epsilon$  and  $\dot{\epsilon}$ , we estimated  $\epsilon$  and  $\dot{\epsilon}$  for all three experiments.

$\tan \delta$  was measured with a Rheovibron at a frequency of 110 cycles/sec. The maximum strain varied from 0.001 to 0.005. Under these conditions the maximum strain rate (i.e., the product of strain amplitude and angular velocity) varies from 0.7 to 3.5  $\text{sec}^{-1}$ .

The modulus measurements were carried out at frequencies between 300 and 600 cycles/sec. The length of samples ranged from 0.3 to 0.4 cm, with the deflection of the fiber amounting to 0.1 cm. Under these conditions the respective ranges of strain and strain rate are 0.12–0.16 and 300–450  $\text{sec}^{-1}$ .

In the measurement of the coefficient of friction, one filament was moved over the other at a rate of 0.1 cm/sec. The monofilaments had a nominal diameter of about 0.002 cm, and the maximum deformation at the point of contact ranged from 0.4 to 0.8 micron, giving the maximum strain amplitude of 0.02–0.04. The length of the area of contact, when the angle between the two filaments is  $30^\circ$ , was calculated to range from 0.0011 to 0.0016 cm. The strain rate during the measurements then ranges from 3.5 to 5.1  $\text{sec}^{-1}$ . The values of strain amplitude and strain rate calculated for the various measurements are given in Table I.

On the basis of these data it can be concluded that in all cases the strain amplitude was sufficiently small and that the properties should be nearly independent of strain. With regard to strain rate, only  $\tan \delta$  and the coefficient of friction were measured under approximately the same conditions. The strain rate for the measurements of modulus was about 100 times higher than that in the determination of the coefficient of friction and  $\tan \delta$ . In order to establish the magnitude of error associated with this difference, we compared the modulus

TABLE I  
Values of Strain Amplitude and Strain Rate for the Various Experimental Methods

Method	Strain amplitude (maximum)	Strain rate (maximum), $\text{sec}^{-1}$
Rheovibron for $\tan \delta$	0.001–0.005	0.7–3.5
Vibroscope for $E$	0.12–0.16	300–450
Gralen's method for friction coefficient	0.02–0.04	3.5–5.1



data  $E$  reported in this article with modulus data determined by the Rheovibron for the nylon 6 fiber. We found that the value of modulus determined by the Rheovibron is about 20% lower than that determined by the vibroscope technique used in the present analysis. The inspection of the results show that this error has a small effect on exponent  $n$ , but it does not affect the general conclusions of this work.

In order to establish the validity of the above equation (within the limits of error associated with the determination of modulus at a higher strain rate) we analyzed the experimental data for nylon 6, PET, polypropylene, and nylon 12 given in Figures 3 to 7. From these results it is possible to extract the values of exponents  $m$  and  $n$  which satisfy the above equation.

The values of the exponents  $m$  and  $n$  for each sample were calculated by solving the simultaneous equations of the type of eq. (3) at various temperatures. Substituting these values of  $m$  and  $n$  in eq. (3), the data can then be plotted as  $\mu$  versus  $(\tan \delta)^m/E^n$  for each fiber. Such plots for nylon 6, PET, polypropylene, and nylon 12 yarn are shown in Figures 10 to 13, where the solid lines represent the least-squares fit through the data points. The values of the exponents  $m$  and  $n$  and those of the intercept  $a$  and slope  $b$ , the latter two as obtained from least-squares analysis, are given in Table II. Included also in this table are values of the standard deviation (S.D.) of data points around the least-squares fit. The agreement of the data with a straight line represented by eq. (3) is excellent, and in each case the value of the intercept  $a$ , although not zero, is very small. It is particularly interesting to note that with nylon 6 and nylon 12 both the temperature and humidity effects are represented by the same values of  $m$  and  $n$ . On the other hand, it is not surprising that  $m$  and  $n$  vary from one fiber to the other.

These results lead to two important conclusions. First, with these fibers the adhesive effect in friction is negligible. This is based on the fact that, the values of intercept  $a$  being very small, the lines of  $\mu$  versus  $(\tan \delta)^m/E^n$  pass almost through the origin.

Second, the changes in fiber morphology resulting from heat treatments, variations in draw ratio, etc., which lead to measurable effects on degree of

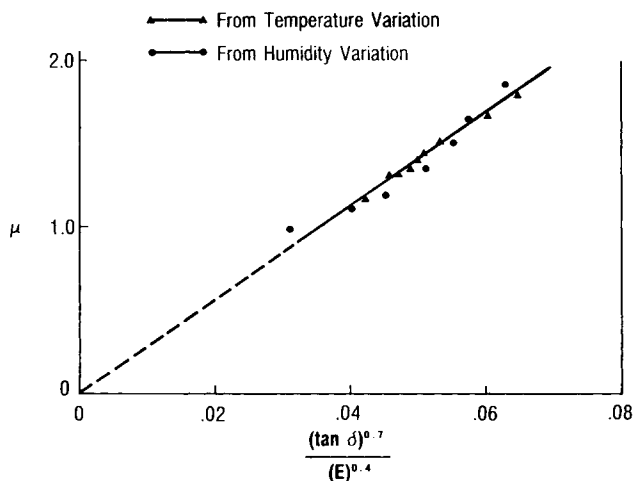
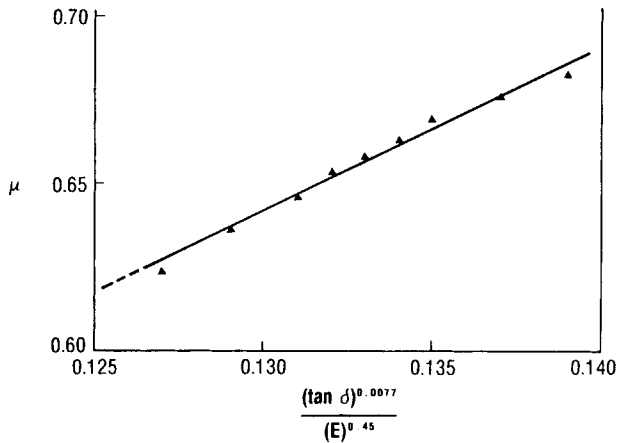
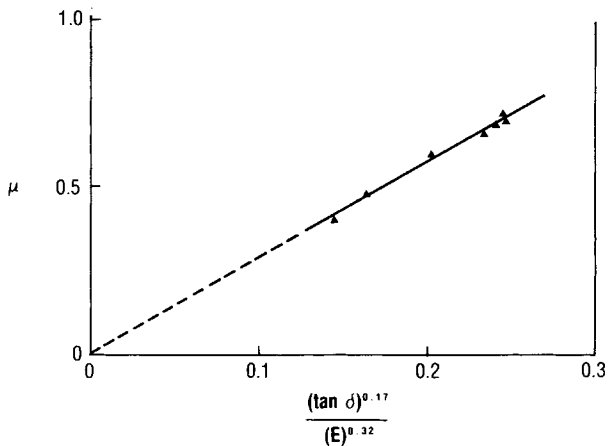


Fig. 10. Variation of  $\mu$  with  $(\tan \delta)/E$  in nylon 6 yarn: ( $\Delta$ ) from temperature variation; ( $\circ$ ) from R.H. variation.

Fig. 11. Variation of  $\mu$  with  $(\tan \delta)/E$  in PET yarn.Fig. 12. Variation of  $\mu$  with  $(\tan \delta)/E$  in polypropylene yarn.TABLE II  
Values of Various Parameters in Eq. (3)

Fiber	Value of exponent		Slope	Intercept	Standard deviation of scatter (S.D.)
	$m$	$n$	$b$	$a$	
Nylon 6	0.700	0.40	26.92	0.060	0.032
PET	0.008	0.45	4.84	0.012	0.002
Polypropylene	0.170	0.32	2.98	0.024	0.010
Nylon 12	0.420	0.35	3.58	0.187	0.015

crystallinity, orientation, etc., will produce only minor effects on the coefficient of friction. Considering that increase in draw ratio always leads to an increase in modulus and frequently to a decrease in  $\tan \delta$ , it can be inferred that the coefficient of friction will usually decrease with increasing draw. The heat setting, on the other hand, will usually lead to an increase in the coefficient of friction. However, the effects are expected to be relatively small. Assume a hypothetical case where a change in fiber process, i.e., an increase in draw ratio, heat setting, etc., leads to an increase of modulus by a factor of 2 and a decrease

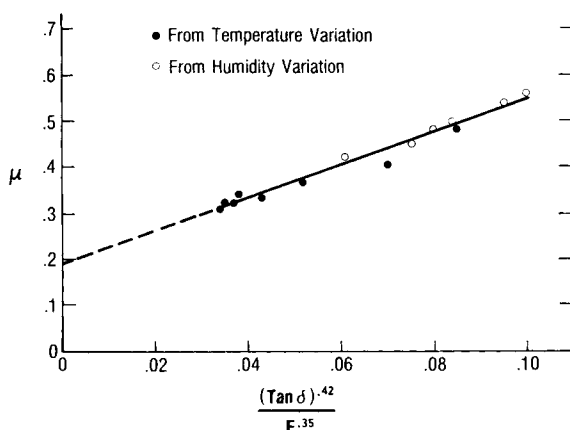


Fig. 13. Variation of  $\mu$  with  $(\tan \delta)/E$  in nylon 12 yarn: (X) from temperature variation; (●) from R.H. variation.

in  $\tan \delta$  by a factor of 1.5, which are rather extreme variations with both  $E$  and  $\tan \delta$  affecting  $\mu$  adversely at the same time. The change in the coefficient of friction estimated by eq. (3) (using average values of  $m$  and  $n$  listed in Table II) is only  $\sim 25\%$ . This result finds support in numerous experimental data indicating that the frictional coefficient of fibers is rather insensitive to variations in fiber morphology. This is different from other properties such as modulus and strength, which can be varied in a much broader range by changes in processing conditions. Thus, it can be inferred that temperature and humidity variations encountered in end uses have a much more important effect on frictional properties than the changes in draw ratio, heat setting, etc.

The present work therefore gives support to the use of  $\mu = a + (b(\tan \delta)^m/E^n)$  in correlating the coefficient of interfiber friction with fiber modulus and  $\tan \delta$ . Nevertheless, it must not be overlooked that values of exponent  $m$  vary from 0.008 for PET to 0.7 for nylon 6. Variations of such magnitude indicate that the relationship between  $\tan \delta$  and  $E$  and the coefficient of friction is more complex than indicated by eq. (3). It is possible that the large variations in  $m$  reflect the dependence of  $m$  on the modulus of the fiber. Note that under a given load the deformation accompanying the sliding motion of a fiber decreases with increasing modulus. It can therefore be expected that the effect of  $\tan \delta$  on  $\mu$  would decrease with increasing modulus. This trend seems to be supported qualitatively by the data investigated in this study.

### References

1. A. Schallamach, *Rubber Chem. Technol.*, **41**, 209 (1968).
2. J. Lindberg and N. Gralen, *Text. Res. J.*, **18**, 287 (1948).
3. G. M. Bartenev, *Dokl. Akad. Nauk USSR*, **96**, 1161 (1954).
4. H. Rieger, *Kaut. Gummi Kunstst.*, **20**, 293 (1967).
5. A. Schallamach, *Wear*, **1**, 384 (1958).
6. A. Schallamach, *Rubber Chem. Technol.*, **39**, 320 (1966).
7. F. P. Bowden and D. Tabor, *The Friction in Lubricating Solids*, Clarendon Press, Oxford, 1954.
8. H. W. Kummer, Pennsylvania State University, *Eng. Res. Bull* **B-94** 1966.
9. K. Minato, C. Nakafuku, and T. Takemura, *Jap. J. Appl. Phys.*, **8**, 1171 (1969).
10. G. V. Vinogradov, Yu. G. Yanovsky, and E. I. Frenkin, *Br. J. Appl. Phys.*, **18**, 1141 (1967).
11. J. A. Greenwood and D. Tabor, *Proc. Phys. Soc.*, **71**, 989 (1958).

12. P. M. Morse, *Vibration and Sound*, McGraw-Hill, New York, 1948.
13. D. C. Prevorsek, R. H. Butler, and G. E. R. Lamb, *Text. Res. J.*, **45**, 60 (1975).
14. D. Bulgin, G. D. Hubbard, and M. H. Walters, *Proc. Fourth Rubber Technol. Conf.*, London, 1962, p. 173.

Received June 22, 1977

Revised September 15, 1977